

RESEARCH

Open Access



# A novel non-Hodgkin lymphoma murine model closer to the standard clinical scenario

Thais Bascuas<sup>1</sup>, María Moreno<sup>1</sup>, Amy Mónaco<sup>1</sup>, Laura Reyes<sup>3</sup>, Andrea Paolino<sup>3</sup>, Patricia Oliver<sup>3</sup>, María G. Kramer<sup>1</sup>, Henry Engler<sup>3</sup>, José P. Pacheco<sup>4</sup>, Sofía Grille<sup>2†</sup> and José A. Chabalgoity<sup>1\*†</sup>

## Abstract

**Background:** Non-Hodgkin lymphomas (NHL) are the most frequent hemato-oncological malignancies. Despite recent major advances in treatment, a substantial proportion of patients relapses highlighting the need for new therapeutic modalities. Promissory results obtained in pre-clinical studies are usually not translated when moving into clinical trials. Pre-clinical studies are mainly conducted in animals with high tumor burden; instead patients undergo chemotherapy as first line of treatment and most likely are under remission when immunotherapies are applied. Thus, an animal model that more closely resembles patients' conditions would be a valuable tool.

**Methods:** BALB/c mice were injected subcutaneously with A20 lymphoma cells and after tumor development different doses of chemotherapy were assessed to find optimal conditions for minimal residual disease (MRD) establishment. Tumor growth and survival, as well as drugs side effects, were all evaluated. Complete lymphoma remission was monitored in vivo using positron emission tomography (PET), and the results were correlated with histology. Immunological status was assessed by splenocytes proliferation assays in NHL-complete remission mice and by analyzing tumor cell infiltrates and chemokines/cytokines gene expression in the tumor microenvironment of animals with residual lymphoma.

**Results:** Two cycles of CHOP chemotherapy at days 25 and 35 post-tumor implantation induced complete remission for around 20 days. PET showed to be a suitable follow-up technique for MRD condition with 85.7 and 75% of sensibility and specificity respectively. Proliferative responses upon mitogen stimulation were similar in animals that received chemotherapy and wild type mice. Tumors from animals with residual lymphoma showed higher numbers of CD4<sup>+</sup> and CD8<sup>+</sup> and similar numbers of NK, neutrophils and Tregs infiltrating cells as compared with non-treated animals. Gene expression of several cytokines as well as an array of chemokines associated with migration of activated T cells to tumor sites was upregulated in the tumor microenvironment of animals that received chemotherapy treatment.

**Conclusions:** We established a NHL-B pre-clinical model using standard chemotherapy to achieve MRD in immunocompetent animals. The MRD condition is maintained for approximately 20 days providing a therapeutic window of time where new immunotherapies can be tested in conditions closer to the clinics.

**Keywords:** Non-Hodgkin lymphoma (NHL), Immunotherapy, Chemotherapy, CHOP, Clinical, Positron emission tomography (PET), Minimal residual disease (MRD)

## Background

Non-Hodgkin lymphomas (NHL) are the most frequent hemato-oncological malignancies. The current standard

of care for NHL treatment is chemotherapy, radiotherapy and monoclonal antibodies (i.e. Rituximab) [1]. Although these combined treatments can achieve high rates of complete remission, a substantial proportion of patients relapses with chemoresistant disease. Survival rates for NHL vary depending on the age, performance status, histological type, stage, (international prognostic index) IPI score and others prognostic factors. According to SEER

\*Correspondence: jachabal@higiene.edu.uy

†Sofía Grille and José A. Chabalgoity share senior authorship

<sup>1</sup> Departamento de Desarrollo Biotecnológico, Instituto de Higiene, Facultad de Medicina, UdelaR, Montevideo, Uruguay

Full list of author information is available at the end of the article

Cancer Statistics Review (CSR), the overall 5-year relative survival rate for all ages is 69%, and the 10-year relative survival rate is 59%; 86% for follicular lymphoma, and 61% for diffuse large B-cell lymphoma (DLBCL) [2].

Active immunotherapy is a promising complementary approach for NHL treatment. Induction of tumor-specific adaptive immunity might generate long-lasting immunological memory able to prevent further relapses, and there is abundant literature demonstrating good rates of effectivity in pre-clinical models [3–5]. However, overall 85% of phase I–II clinical trials for novel treatments in cancer fail; and of those that progress to phase III, only half become approved for clinical use [6]. Pre-clinical NHL active immunotherapy studies are mainly performed in mice with high tumor burden that received no previous treatment, whereas clinical trials are performed in patients that have undergone chemotherapy and they are in complete or partial remission [3, 7]. Thus, murine models usually do not resemble the clinical scenario and this can be a major reason to explain the lack of consistency in results when moving into clinical trials [8]. The development of novel pre-clinical models that mimic the clinical setting could be valuable tool to explore new therapeutic strategies [9]. Particularly, it would be important to have a model in which animals achieved complete remission with chemotherapy and develop minimal residual disease (MRD) state.

We have previously assessed a murine NHL-B model where different immunotherapies were evaluated with promising results [10–12]. In the present study, we establish a new NHL-B pre-clinical model using standard chemotherapy (CHOP) to achieve complete response in immunocompetent animals. We believe that this model is more suitable to study new and optimized immunotherapies, thus it could be a valuable tool for pre-clinical studies that get closer to the clinics.

## Methods

### Animals and tumor cell line

Female BALB/c mice, 8–10 weeks old were used for in vivo experiments. Animals were housed on a 12:12 h light/dark cycles in racks with filtered air where food and water were given ad libitum.

The A20 cell line was derived from B lymphocytes of a naturally occurring reticulum cell sarcoma from an old BALB/cAnN mouse and was obtained from the American Type Culture Collection (Manassas, VA, USA). Cells were grown in RPMI-1640 medium (Sigma-Aldrich, St. Louis, MO) supplemented with 10% fetal bovine serum (PAN-Biotech, Aidenbach, Germany), 2 mM L-glutamine (Sigma) and 0.05 mM 2-mercaptoethanol (Sigma-Aldrich, St. Louis, MO) (RPMI complete medium) at 37 °C in 5% CO<sub>2</sub> atmosphere.

### Cell transplantation

For tumor challenge, A20 were grown in culture and harvested in log phase, washed and resuspended to a final concentration of  $5 \times 10^6$  cells/ml in PBS. 8–10 weeks-old syngeneic female BALB/c mice were injected subcutaneously (s.c.) into the right flank with  $1 \times 10^6$  cells in 0.2 ml of PBS. Tumors were measured three times a week with a microcaliper in three dimensions, and tumor volumes were calculated as length  $\times$  width  $\times$  depth  $\times$  0.5236, as previously described [13]. Mice were euthanized by cervical dislocation when tumors reached 3000 mm<sup>3</sup> or before if they showed signs of distress. These time points were defined as survival time.

### Chemotherapy treatment for MRD lymphoma model

The standard chemotherapy regimen in patients for aggressive NHL as well as the most used regimen for indolent NHL is a combination of cyclophosphamide, doxorubicin, vincristine and prednisone/steroids (CHOP) given every 21 days for 6–8 cycles [1, 14]. We used a CHOP regimen to treat mice bearing lymphoma where oral prednisone was substituted by intraperitoneal (i.p.) dexamethasone in order to achieve more uniform levels of steroid and to reduce chemical peritonitis. In each chemotherapy cycle we used the following doses: cyclophosphamide 100 mg/kg i.p., doxorubicin 6 mg/kg i.p., vincristine 0.1 mg/kg i.p. and dexamethasone 0.2 mg/kg i.p. At day 25 post-tumor implantation (p.t.i.), groups of mice ( $n = 9$ ) that were inoculated with A20 cell line were treated either with one cycle of chemotherapy (CHOP $\times$ 1), two cycles of chemotherapy (CHOP $\times$ 2) or PBS as control and were followed for tumor growth and survival. Side effects were monitored, through weight changes evaluation and hematological toxicity. Lymphocytes, monocytes and neutrophils recovery post-CHOP were evaluated in an automated blood cell counter and in peripheral blood smears. Blood was obtained using a 27G needle puncturing the tail vein. This allows us to select the optimal period between CHOP cycles.

To avoid potential infections, prophylactic anti-infectious drugs (15 mg/kg of fluconazole and 20 mg/kg of acyclovir) were used during the neutropenia period.

### Chemotherapy cytotoxicity

Cytotoxic effect of CHOP drugs on A20 tumor cell line was assessed in vitro by growth inhibition studies. Cells were seeded in 24-well plates at a density of  $1 \times 10^6$  viable cells per well. Triplicate wells were treated with different concentrations of the drugs or PBS and Dimethyl sulfoxide (DMSO) as controls (Sigma-Aldrich, St. Louis, MO). Cyclophosphamide, doxorubicin, and dexamethasone were tested 0.1, 1, 10, 100 nM and 1  $\mu$ M, and Vincristine was tested 10, 20, 30, 40, 50 and 70 nM. Plates

were incubated at 37 °C in a humidified incubator with 5% CO<sub>2</sub> for 96 h. Then, all cultures were monitored for cell viability using Trypan blue vital stain (Life Technologies, Carlsbad, CA), and Annexin V (BD Pharmingen, San Diego, CA) with Propidium iodide (PI) (Sigma-Aldrich, St. Louis, MO). The half maximal inhibitory concentration (IC<sub>50</sub>) was calculated as the concentration (nM) that causes half of the cell mortality.

To evaluate *in vivo* toxicity, body weight was measured before and after CHOP administration. The body weight change (BWC) was calculated using the following formula:  $BWC (\%) = \frac{[(\text{body weight on the last day}) - (\text{body weight on day 0})]}{(\text{body weight on day 0})} \times 100 (\%)$ , as previously described [15].

### Necropsy and histology

Mice were sacrificed at day 45 p.t.i. and necropsies were performed. Animals were examined macroscopically for lymphoma infiltration at primary sites or lymph nodes or other organs. Primary lymphoma site, inguinal and retroperitoneal lymph nodes, liver and spleen were removed and immersed in formalin buffered 10% at room temperature for 24 h. Organs were washed with PBS for 24 h at 4 °C and then immersed successively two times for 2 h in EtOH 95%, absolute alcohol, Xylol, paraffin and processed in paraffin blocks. Sections of 4 μm were cut and dewaxing immersed successively two times for 5 min in xylol and absolute alcohol, one time for 5 min in EtOH 95% and EtOH 90%. Then sections were washed three times with distilled water and stained with hematoxylin-eosin. Finally, sections were immersed successively for 3 s in EtOH 70%, EtOH 80%, EtOH 95%, absolute alcohol and Xylol, and assembled with Canada balsam. These sections were microscopically evaluated to detect lymphoma infiltration.

### PET/CT imaging

Complete lymphoma remission was evaluated by *in vivo* imaging using positron emission tomography/computed tomography (PET/CT) scan with <sup>18</sup>F-2-fluor-2-desoxy-D-glucosa (<sup>18</sup>F-FDG) as radiotracer. The study was performed in the Centro Uruguayo de Imagenología Molecular (CUDIM).

### Image acquisition

PET/CT imaging in mice was performed using a tri-modality scanner (Triumph, Trifoil, Inc., US) with LYSO/LGSO scintillators (spatial resolution: 1.0 mm and an axial field of view: 3.75 cm). Data were acquired in list mode in a 184 × 184 × 31 matrix with pixel size: 0.25 × 0.25 × 1.175 mm; coincidence window width: 22.22 s.

Seventeen mice were evaluated by PET/CT, of which two died later on as result of cytotoxicity and thus were excluded from the analysis. Images were obtained before (day 25 p.t.i.) and after CHOP treatment when mice were in complete clinical remission (day 44 p.t.i.). The animals were anesthetized with 2% isoflurane in an oxygen flow of 2 l/min, placed in prone position on the scanner bed and injected via the caudal vein with 100 μl of (<sup>18</sup>F-FDG) (20 ± 5.4 MBq). PET images (static studies) acquisition started 30 min after radiotracer administration and performed over 60 min. Sinograms were reconstructed using 3D maximum likelihood expectation maximization (3D-MLEM).

### Image analysis

Semi-quantitative analysis was done using PMOD software version 3.4 (PMOD Technologies, Ltd., Zurich, Switzerland). PET studies were co-registered with the corresponding CT scan studies for anatomical localization. Images were displayed as coronal, sagittal and axial slices.

For quantifying the specific uptake, volumes of interest (VOIs) were drawn manually on tumor as target (T) and skeletal muscle as non-target tissue (NT) [16]. The activity uptake was expressed as KBq/cc; results were expressed as T/NT.

### Splenocyte proliferation assay

At day 45 p.t.i. mice in complete remission from CHOP×2 group as well as mice from PBS control were sacrificed and spleens were removed. Spleens were disrupted and prepared as a single-cell suspension. Splenocytes were stained with 1 μM of 5(6)-carboxyfluorescein diacetate *N*-succinimidyl ester (CFSE) (Sigma-Aldrich, St. Louis, MO). CFSE labeled splenocytes were incubated at 37 °C with 5% CO<sub>2</sub> in 24 wells plate at 2 × 10<sup>6</sup> cells/ml density by triplicates in complete medium for 4 days and were stimulated with 1 μg/ml of Concanavalin A (ConA) (Sigma-Aldrich, St. Louis, MO) or non-stimulated. After the incubation, cells were washed and stained with PI for 10 min in the dark at room temperature. Data were acquired by flow cytometry (FACS Canto II, Becton–Dickinson) and were analyzed with ModFit software (Verity Software House, Inc). For analysis, viable cells were gated based on FSC and PI profiles. The parent generation was set as the median fluorescence intensity using non-stimulated control sample.

### Flow cytometry analysis of tumor-infiltrating cells

At day 45 p.t.i. mice with residual primary lymphoma from CHOP×2 group (i.e. animals with partial response to chemotherapy) as well as PBS control, were sacrificed

and tumors were removed and prepared as a single-cell suspension. Cells were immunostained at 4 °C in the dark for 30 min with the following panel of antibodies: FITC-conjugated anti-CD49b, PEcy7-conjugated anti-CD8, APC-conjugated anti-CD3, APCCy7-conjugated anti-CD4, PerCPCy5.5-conjugated anti-CD19, FITC-conjugated anti-CD4, PE-conjugated anti-FoxP3, PEcy7-conjugated anti-CD3, APC-conjugated anti-CD25, FITC-conjugated anti-Ly6C, PE-conjugated anti-Ly6G, (all reagents from BD Pharmingen, San Diego, CA). Optimal antibody concentration was previously defined by titration. For intracellular FoxP3 staining, cells were first stained with anti-CD4 and anti-CD25 antibodies, then fixed and permeabilized with a mouse FoxP3 buffer set (BD Pharmingen) according to the manufacturer's protocols. Cells were washed twice with permeabilization buffer and then incubated with anti-FoxP3 at 4 °C for 30 min in the dark. Flow cytometry data were collected on a FACS Canto II flow cytometer equipped with two lasers (Becton–Dickinson, Oxford, UK). For data acquisition and analysis, FACSDiva (Becton–Dickinson) and Infinicyt (Cytognos, Spain) software were used.

#### Determination of cytokines and chemokines in tumor microenvironment

Tumor microenvironment cytokines and chemokines mRNA levels were determined using quantitative reverse transcription-PCR. At day 45 p.t.i mice from PBS and CHOPx2 group, in which primary tumor persisted (partial remission), were sacrificed and tumors were removed, immersed in Trizol reagent (Invitrogen, Carlsbad, CA) and stored at –80 °C until processed. Tumors were homogenized with an Ultra Turrax T8 homogenizer (IKA-Werke, Staufen, Germany) and RNA was extracted according to the manufacturer's instructions. RNA quality and quantity were assessed by spectrophotometric measurements at 260/280 nm in a NanoDrop 2000 (Thermo Fisher Scientific, Waltham, MA). Before cDNA synthesis, 1 µg total RNA was treated with DNase I (Invitrogen), and first-strand cDNA synthesis was carried out using random primers (Invitrogen) and Moloney murine leukaemia virus reverse transcriptase (Invitrogen). Real-Time PCR (RT-PCR) was performed using a QuantiTect SYBR green PCR kit (Qiagen, Hilden, Germany) in a 7900HT RT-PCR System (Applied Biosystems, Foster City, CA). *B2m* gene was used as housekeeping gene. The primers used are listed in Table 1 and were used at a final concentration of 0.9 µM. The relative mRNA amount in each sample was calculated using the  $2^{-\Delta\Delta Ct}$  method [17], where  $\Delta Ct = Ct_{\text{gene of interest}} - Ct_{B2m}$  and expressed as relative mRNA levels in the test group compared with the control group (fold change).

#### Statistical analysis

Results were analyzed in SPSS 17.0 (Statistical Package for the Social Sciences) for Windows. Differences in survival times were determined using Kaplan–Meier and log-rank test. For tumor growth and in vitro assays the statistical significance of differences between study groups were analyzed using Student's t-test and analysis of variance (ANOVA). A value of  $p < 0.05$  was considered statistically significant.

Receiver operating characteristic curve (ROC) was used to evaluate the T/NT ratio in the diagnosis of complete remission by assessing the area under the ROC curve (AUC), sensitivity, and specificity. The cut-off point was determined by maximizing the sum of sensitivity and specificity; histology was used as a gold standard variable.

## Results

#### Chemotherapy efficacy and in vivo toxicity

First, we assessed the bioactivity of the cytostatic drugs on the A20 tumor cell line. The in vitro  $IC_{50}$  values obtained for doxorubicin and vincristine were 25 and 1 nM respectively, which are similar to the reported  $IC_{50}$  values of these two drugs on other tumor-sensitive cell lines, confirming the possibility of using them on the lymphoma model. Our results also confirmed that cyclophosphamide and dexamethasone cannot be evaluated in vitro since they both requires hepatic activation [18].

We then treated A20-bearing animals with increasing doses of CHOP starting with doses used in a previously reported xenograft lymphoma model [19]. Those particular doses did not show any anti-tumor effect on A20-bearing immunocompetent animals, so we doubled them and found that they were too toxic and all animals succumbed to the treatment (results not shown). Thus, we decided to assess intermediate values and to apply two cycles separated ten days apart. This interval between cycles was decided based on results from white blood cells peripheral count that demonstrated complete bone marrow regeneration at day 10 post-chemotherapy. Overall, these studies provided us with an optimal CHOP doses regime for treatment as described in Methods. At these particular doses, animals had an acceptable tolerance to chemotherapy. Particularly, no animals died with one cycle of CHOP, while 18% of animals receiving two cycles of CHOP died by chemotherapy cytotoxicity. Low levels of toxicity were also evidenced by variations in body weight over time (Fig. 1a). The highest decrease in weight was observed ten days after second CHOP cycle, and after that, animals started to recover towards average normal body weight. Cachexia was not observed at any time after CHOP administration. Transient neutropenia and monocytopenia were observed post CHOP, but

**Table 1 Sequences of primers used for quantitative RT-PCR**

Gene	Forward primer (5'–3')	Reverse primer (5'–3')	Product length (bp)
<i>B2m</i>	CCTGCAGAGTTAAGCATGCCAG	TGCTTGATCACATGTCTCGATCC	72
<i>Ccl2</i>	CCCTCAACGGGAAGAACCAAA	CACATCAGGTACGATCCAGGC	72
<i>Ccl3</i>	AACATCATGAAGTCTCCAC	CCAAGACTCTCAGGCATTCA	294
<i>Ccl4</i>	GCCCTCTCTCTCTCTTGCT	GTCTGCCTCTTTTGGTCAGG	196
<i>Ccl5</i>	GGTACCATGAAGATCTCTGCA	AAACCCTCTATCTAGCTCAT	294
<i>Ccl20</i>	TTTTGGGATGGAATTGGACAC	TGCAGGTGAAGCCTTCAACC	69
<i>Cxcr4</i>	TTCTCATCTGGCCTTCATC	CTTTTCAGCCAGCAGTTTCC	92
<i>Cxcr7</i>	GCCGTACCATTTTGTGGTTC	TGCAACGCTGTAAAGAGCAC	96
<i>Cxcl1</i>	CTTGTTTCAGAAAATTGTCCAAA	ACGGTGCCATCAGAGCAGTCT	84
<i>Cxcl9</i>	TGGAGCAGTGTGGAGTTCGA	CCTCGGCTGGTGTGATG	73
<i>Cxcl10</i>	GCCGTCAATTTTGCCTCAT	GCTTCCCTATGGCCCTCATT	127
<i>Cxcl11</i>	CAAAATGGCAGAGATCGAGAAA	TGAGCCTTCATAGTAACAATCACTTCA	87
<i>Cxcl12</i>	GAAGTGGAGCCATAGTAATGCC	TCCAAGTGAAAAAATACCCG	133
<i>Cxcl13</i>	CAACTGTTGTCGGTCTAAACATCAT	GGTCCAGATCACAACCTCAGTTTTG	89
<i>Gal-1 (Galectina-1)</i>	TGAACCTGGGAAAAGACAGC	TCAGCCTGGTCAAAGGTGAT	190
<i>Il2</i>	CCTGAGCAGGATGGAGAATTACA	CTTTCAATTCTGTGGCCTGCTTGGG	92
<i>Il4</i>	ACAGGAGAAGGGACGCCAT	GAAGCCCTACAGACGAGCTCA	95
<i>Il6</i>	GTTCTCTGGGAAATCGTGAAAA	AAGTGCATCATCGTTGTTTACATA	78
<i>Il10</i>	CATTTGAATTCCTGGGTGAGA	TGCTCCACTGCCTTGCTCTT	101
<i>Il12</i>	ATCACACGGGACCAAACCA	CAGGCAACTCTCGTTCTTGTTAGT	74
<i>Il17a</i>	CTCCAGAAGGCCCTCAGACTAC	GGGTCTTCATTGCGGTGG	69
<i>Ifng</i>	TCAGCAACAGCAAGGCGAAA	CCGCTTCTGAGGCTGGAT	143
<i>Tgfb</i>	GCTGAACCAAGGAGACGGAAT	GAGTTTGTATCTTTGCTGTACAAGA	76
<i>Foxp3</i>	CCCAGGAAAAGACAGCAACCTT	TTCTACAACCAGGCCACTTG	89
<i>Tnfa</i>	CATCTCTCAAAATTCGAGTGACAA	CCTCCACTTGGTGGTTTGCT	63

normal values were recovered by day 10–15. Both CHOP cycles induced transient myelosuppression (Fig. 1b). Instead, lymphocytes levels in blood also decreased after CHOP, and values did not return to previous values within the time frame of the experiments.

All in all, these results showed that we had found a suitable chemotherapy treatment with reasonable toxicity levels.

#### Tumor development and survival rate

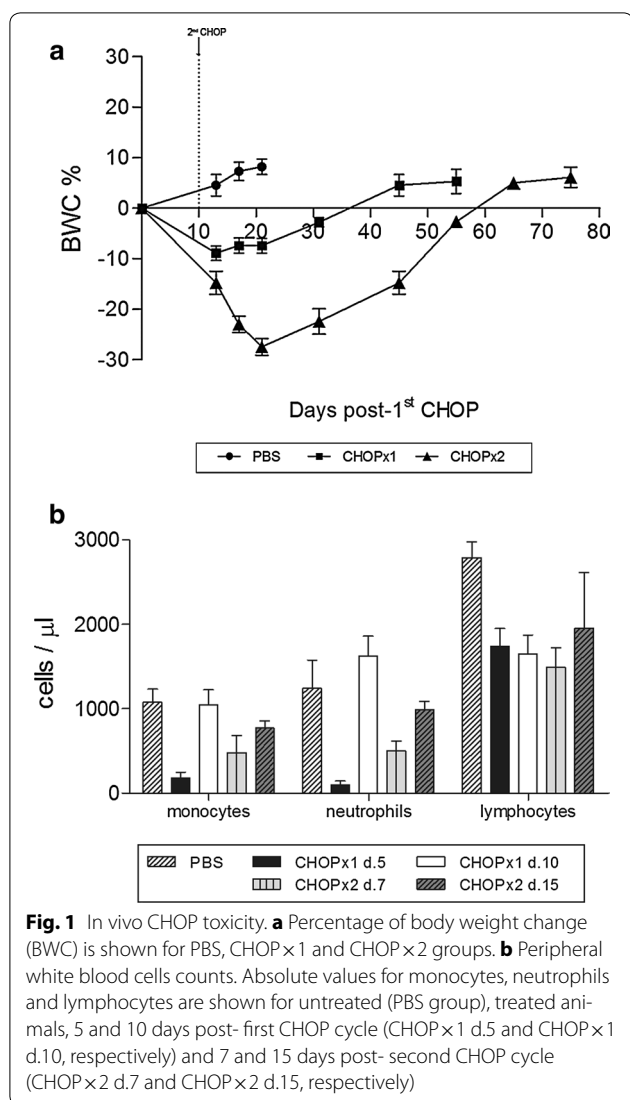
We then evaluated the effect of the selected CHOP regimen on tumor development and survival. As previously shown by us [10], A20-bearing animals that do not receive any treatment show sustained tumor growth over time and a median survival of around 35 days. On the contrary, animals receiving either one or two doses of chemotherapy showed a decrease in tumor growth from day 25 p.t.i., starting immediately after the first CHOP cycle (Fig. 2a). Mice receiving a single CHOP dose had a period when tumor volume decreases and it was close to zero, but this status lasted only for a few days. Instead, in the group of animals receiving two doses of CHOP, around 92% of animals showed clinical complete

remission of the primary tumor for a longer period of approximately 20 days (Fig. 2a, b). After that tumors started to grow again and eventually all mice died for lymphoma disease. Reasons of death among the animals depended of the particular treatment group and were either drug toxicity or respiratory distress, most likely due to metastasis, or the animals where euthanized for ethical reasons when the tumor reached a pre-defined volume size of 3000 mm<sup>3</sup> (Table 2). Survival among animals receiving any chemotherapy regimen was extended, but it was significantly higher among animals receiving two cycles of chemotherapy (Fig. 2c).

#### Evaluation of remission in treated animals

##### Histology

A major aim of our work was to develop a lymphoma MRD model as a more suitable model for immunotherapy assessment. For this, we treated the animals with two doses of CHOP and achieved complete clinical remission during a period of around 20 days. To confirm complete remission in these animals, five mice per group were euthanized at day 45 p.t.i. to perform necropsies and histological analysis. Macroscopically, control animals (no



treatment) showed disseminated disease with extensive lymph nodes and/or hepatic involvement (Fig. 3a). There were lymphoma infiltrations at inguinal and retroperitoneal lymph nodes. Instead, CHOPx2 animals did not show any disseminated disease (Fig. 3b). We also evaluated by histology the primary tumor site, draining lymph nodes, retroperitoneal lymph nodes, spleen, liver and other tissues of abnormal appearance in order to evaluate lymphoma infiltration. Hematoxylin-eosin stained sections demonstrated tumor tissue consisting of a diffuse growth pattern with large and cohesive tumor cells with pleomorphic nuclei resembling centroblast and some small/medium size centrocyte-like cells. Numerous small vessels (capillaries and arterioles) were visible among the tumor cells (Fig. 4). These cells were histological similar to human DLBCL. Liver involvement was 76 and 11% for

control and CHOPx2 groups respectively as evaluated by histology. Liver lymphoma infiltration was characterized by atypical large lymphoid cells with central perivascular distribution within the liver parenchyma (Fig. 4d).

**PET-CT evaluation**

Advanced imaging techniques can improve disease assessment, not least because they allow response evaluation to treatment and follow-up without the need of sacrificing animals. We evaluated PET as an alternative for in vivo monitoring of the disease. For this, we first demonstrated glucose analogue (<sup>18</sup>F-FDG) uptake by A20 lymphoma cells in tumor-bearing mice confirming that <sup>18</sup>F-FDG was a good radiotracer for PET imaging in A20 model.

PET-CT imaging was performed before (day 25 p.t.i.) and after (day 45 p.t.i.) CHOP treatment in order to evaluate <sup>18</sup>F-FDG uptake and to confirm the complete remission (MRD negative status). Post-chemotherapy, T/NT cut-off value was set to 2.45 and calculated using a ROC curve with histology as a gold standard. T/NT values of 2.45 or more were considered residual lymphoma disease. The AUC reached 0.74 (95% CI 0.6–0.991), with a sensitivity of 85.7% and specificity of 75%. Considering this cut-off value, pre-CHOP imaging (day 25 p.t.i.) indicated primary tumor uptake without metastasis as expected (Fig. 5a). On the other hand, post-CHOP PET image analysis (day 45 p.t.i.) revealed complete remission in many animals (Fig. 5b). Other mice had uptake at the site of the primary tumor (Fig. 5c), in disagreement with the histology result, suggesting the existence of false positive. Animals that had residual primary tumor after CHOPx2 treatment also presented retroperitoneum and liver <sup>18</sup>F-FDG uptake (Fig. 5c) evidencing the existence of metastasis in accordance with histology results.

**Immunological status after chemotherapy treatment**

In order to assess the immunological status of CHOP-treated animals, five mice per group were sacrificed at day 45 p.t.i. and spleens were removed for proliferation assays. As shown in Fig. 6, mice in complete remission showed similar proliferation rate upon mitogen stimulation than control mice (PBS).

Additionally, mice with residual lymphoma (partial response) post CHOPx2 treatment were also sacrificed at day 45 p.t.i., and the primary tumor was removed to evaluate tumor-infiltrating populations. Animal from CHOPx2 group showed significantly higher numbers of CD4<sup>+</sup> (p = 0.0023) and CD8<sup>+</sup> (p = 0.0034) tumor-infiltrating T cells as compared with animals from the control group (Fig. 7). Numbers of NK cells, regulatory T cells

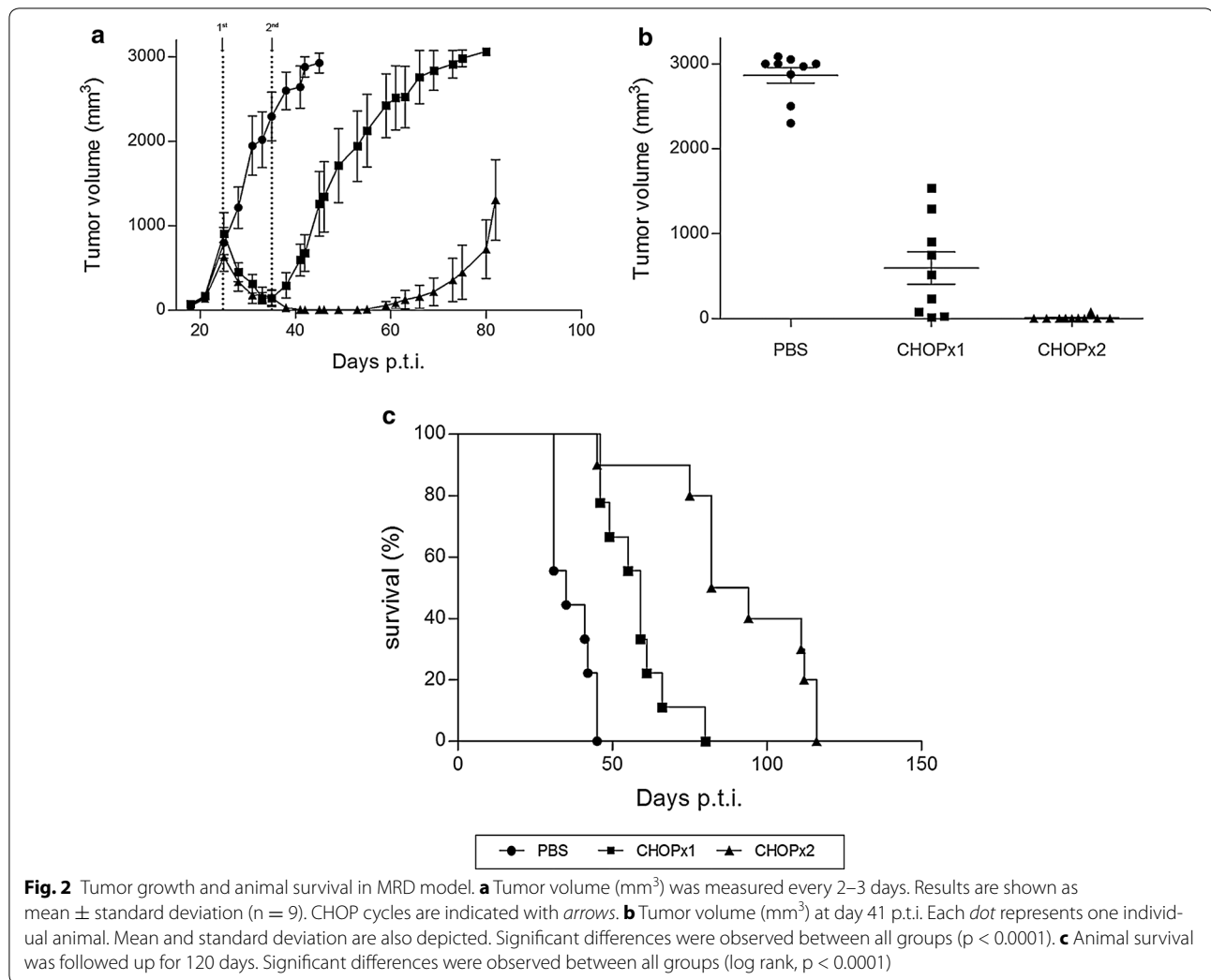


**Table 2** Percentage of animal death related to drug resistance, metastatic disease and primary tumor

	PBS	CHOPx1	CHOPx2
Drug toxicity	NA	0%	18%
Metastatic disease	0%	25%	47%
Primary tumor (>3000 mm <sup>3</sup> )	100%	75%	35%

NA not applicable

(Treg) and neutrophils cells in the tumors were similar in treated and non-treated animals. Analysis of cytokines and chemokines mRNA levels in the tumor microenvironment of animals with partial response to chemotherapy showed significant increases in mRNA levels for *Ccl3*, *Ccl4*, *Ccl5*, *Cxcl9*, *Cxcl12*, *Il2*, *Il12* and *Ifng* whereas *Cxcr4* and *Tgfb* gene expression were significantly repressed as compared with tumors from untreated mice (Fig. 8).

### Discussion

Therapies against NHL have achieved substantial success in the last few years [2, 3], but rates of relapse are still high fostering the research on new therapeutic approaches. Animal models are essential for research and development of novel immunotherapies, and the use of well-characterized inbred laboratory mice is most likely one of the best experimental systems for cancer research. Cancer development has similar physiologic characteristics in mice and humans with the acquisition of mutations in equivalent oncogenes and suppression genes [20, 21]. Xenograft models are widely used to demonstrate pre-clinical activity of drugs prior clinical evaluation, but they are not adequate for testing immunotherapies or studying tumor microenvironment because these require immunocompetent mice [9]. Also, in order to more accurately predict human responses NHL immunotherapies should be tested in a similar context to that usually found

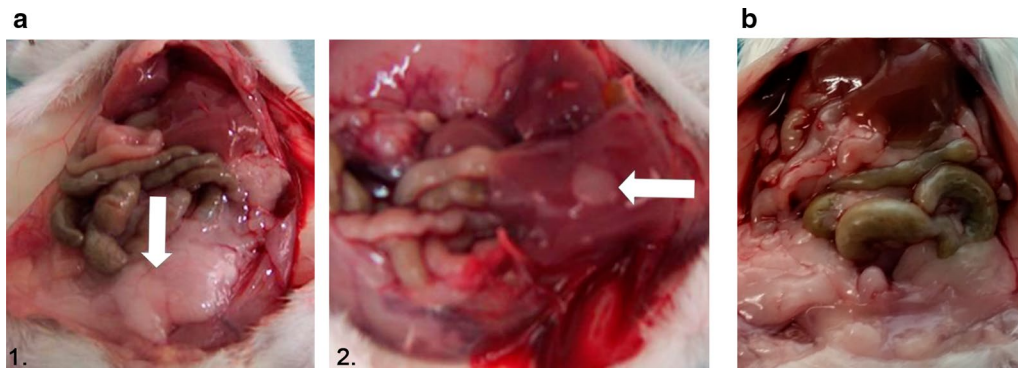


**Fig. 3** Necropsy of chemotherapy-treated and untreated animals at day 45 p.t.i. **a** Untreated mouse: retroperitoneal (1) and hepatic (2) involvement are indicated with arrows. **b** CHOP x2-treated mouse in complete remission

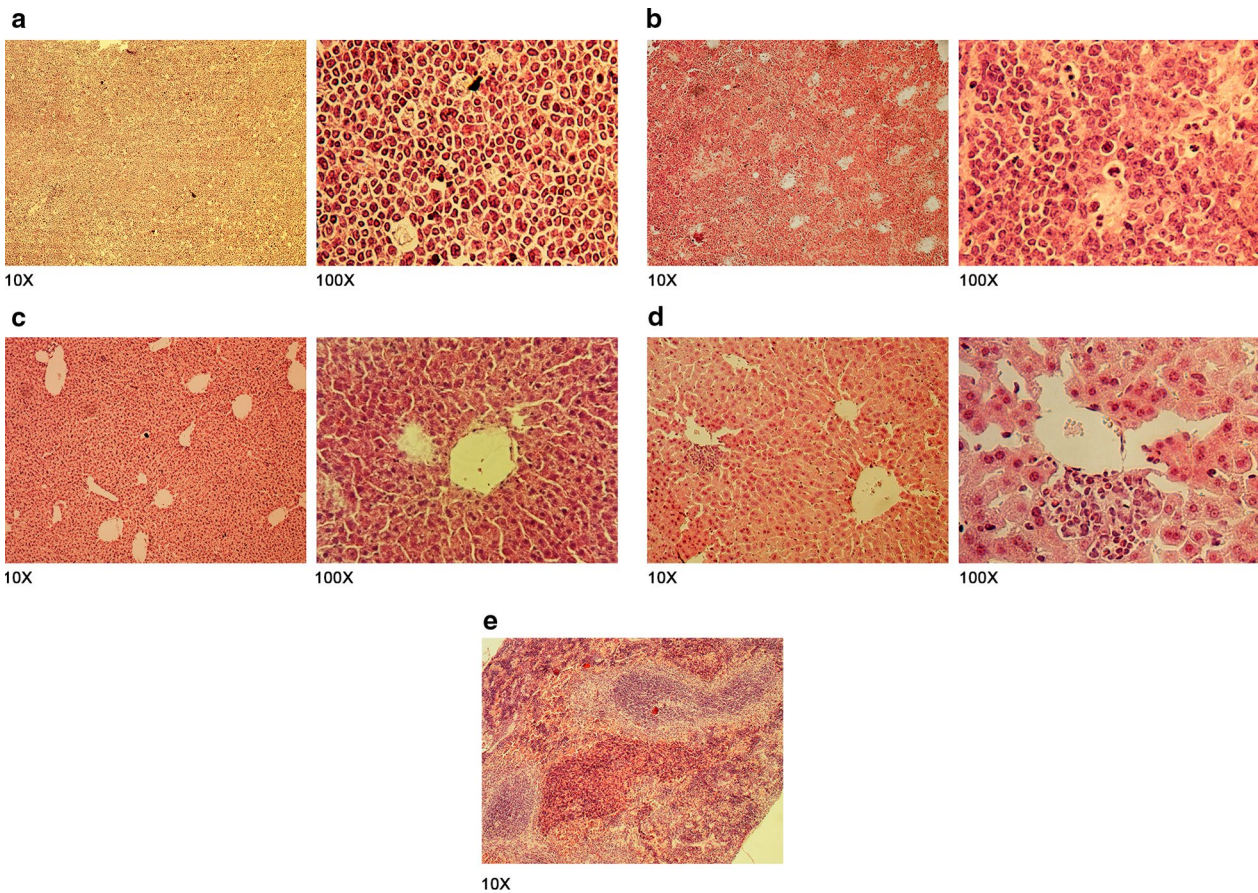
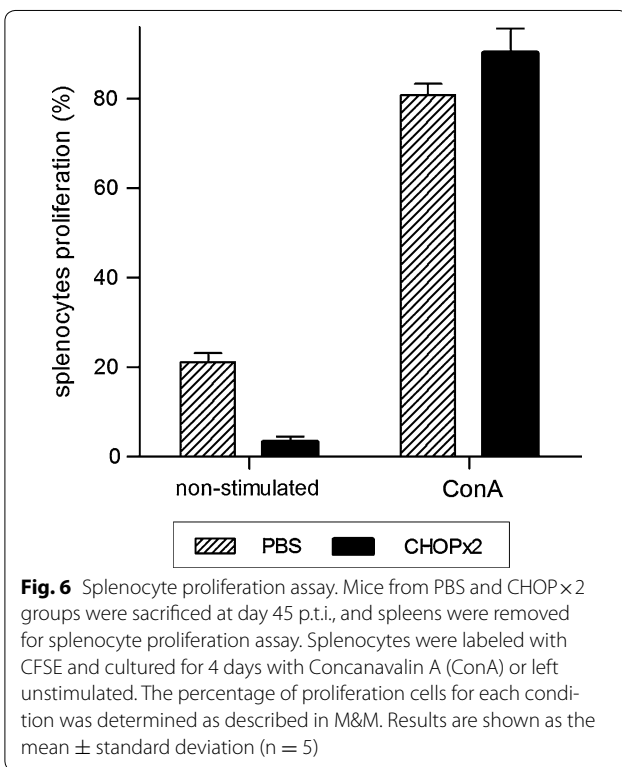
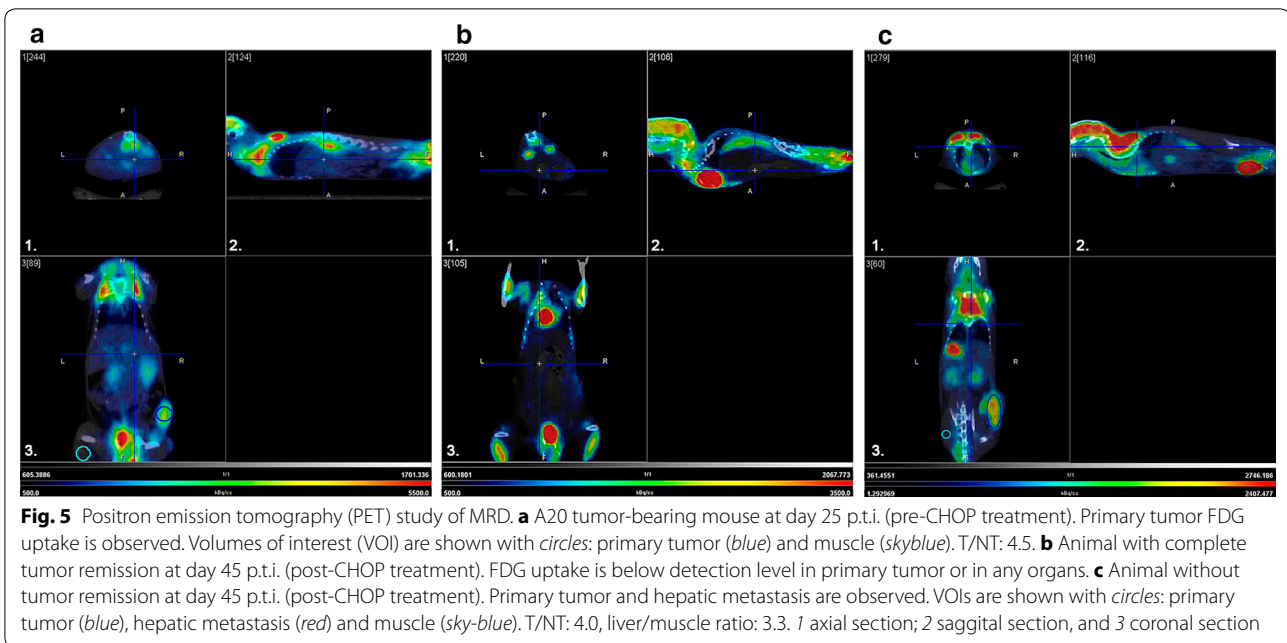


**Fig. 4** Histological study of MRD. **a** Primary tumor sections from a control mouse (PBS group): NHL-B histology is observed and corresponds to a diffuse infiltration by centrocytes and centroblasts with a starry sky pattern, due to high proliferation rate. **b** Retroperitoneal sections from a mouse where NHL disease persists post-chemotherapy: similar histology of primary tumor is observed. **c** Liver sections from a mouse with complete remission: typical healthy hepatic architecture with the centrilobular veins and hepatic sinusoids is observed. **d** Tumor-infiltrated liver sections from a mouse where NHL disease persists post-chemotherapy: infiltrating tumor cells are observed in portal field. **e** Spleen section from mouse with complete remission: normal architecture with the white and red pulp is observed

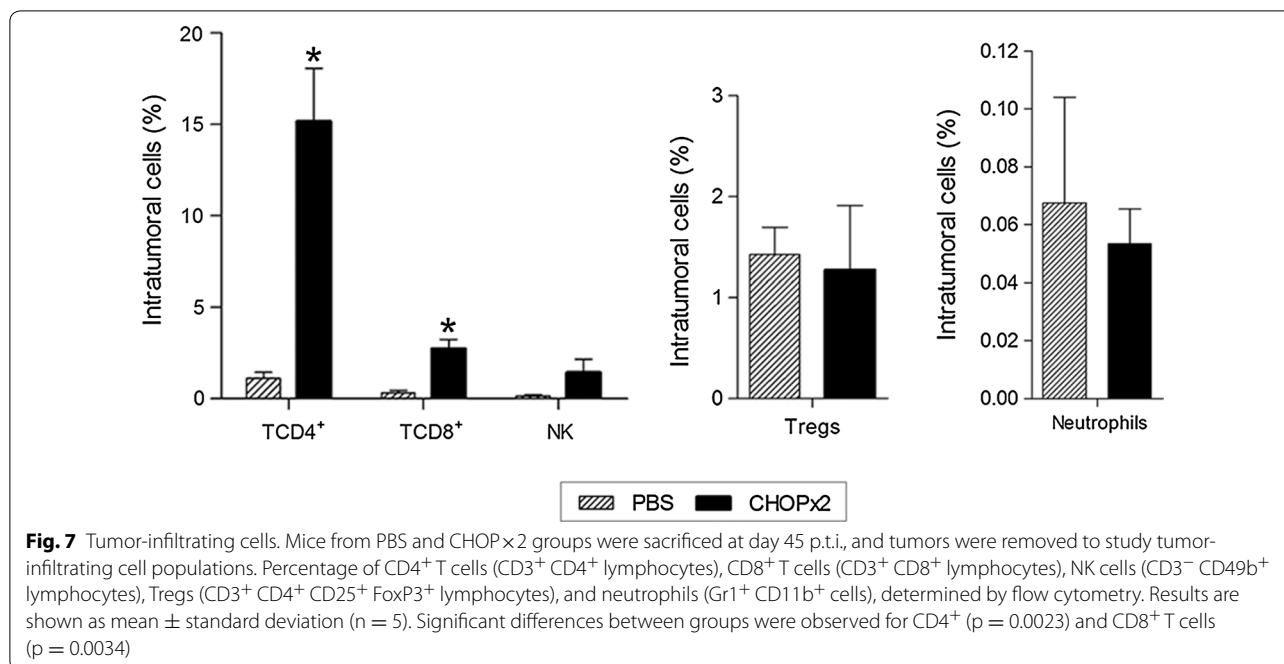


in humans, which for most of the cases implies chemotherapy-treated patients. Chemotherapy can modulate distinct features of tumor immunobiology and the optimal integration of immunotherapies with standard chemotherapies to minimize antagonistic interactions

and engage potential synergies is a major challenge [22]. Ideally, immunotherapy should be applied in the setting of MRD, after the tumor mass has been reduced with systemic chemotherapy. This strategy should minimize the negative impact of tumor bulk on the immune response and might work potentiating the immunological effects of chemotherapy. Indeed, the use of immunotherapy associated with traditional agents, as combination therapy, is now the standard for treatment of many types of cancer, improving clinical outcomes.

Many clinical trials with vaccines against NHL have shown anti-tumoral responses after achieving complete or partial remission with chemotherapy [3, 5, 23, 24]. For all these reasons, we propose that pre-clinical investigation in NHL should be attempted in a murine model that mimics that clinical setting.

The four-drug combination CHOP (cyclophosphamide, doxorubicin, vincristine, and steroids) with Rituximab has become the “standard” first line treatment for aggressive NHL (most frequently diffuse large B cell lymphoma) and it is the most used regimen for treat indolent lymphoma [1, 14, 25, 26]. In order to define more suitable pre-clinical conditions, we assessed the use of CHOP to generate a new model in A20-bearing animals that more closely resemble the clinical scenario. First, we tested the in vitro sensitivity of A20 cells to CHOP drugs. We found that the IC<sub>50</sub> for doxorubicin and vincristine in A20 cells were similar to those reported by DiJoseph et al. in other lymphoma cell line [18]. Since cyclophosphamide and dexamethasone could not be evaluated because they require hepatic activation, we then tested



the combination of drugs in vivo in A20-bearing animals, and found that a two-cycles drug schedule induces lymphoma remission for at least 20 days (MRD status) in a highly reproducible way. This schedule was well tolerated with transient and mild neutropenia and body weight loss.

We also found that administration of chemotherapy did not result in immunosuppression in A20-bearing animals. Cancer chemotherapy was historically considered as promoting immunosuppression, but recent studies have demonstrated that certain chemotherapies can instead augment tumor immunity in addition to their cytotoxic effect. Chemotherapy can promote anti-tumor immune responses by increasing the immunogenicity of malignant cell, or by inhibiting immunosuppressive circuits that are established by cancer [27–29]. Some chemotherapy drugs at their standard dose mediate their tumor effect, at least in part, by inducing immunogenic cell death, which involves the release of tumor antigens and danger-associated molecular patterns (DAMPs) in the tumor microenvironment, resulting in a proinflammatory microenvironment, where specific anti-tumor immunity may be developed [28]. It has also been demonstrated that chemotherapy can modulate the activity of immune T-cell subsets decreasing the number of Tregs cells, shifting CD4<sup>+</sup> T helper phenotype from type 2 to type 1, inducing the differentiation of Th17 cells, and promoting the evolution of a durable T-cell memory [28]. We found that animals receiving the two CHOP doses (CHOPx2 group) have higher numbers of CD4<sup>+</sup> and

CD8<sup>+</sup> T cells recruited to the tumor as well as a significant increase in *Il12* and *Ifng* and a decrease in *Tgfb* gene expression reinforcing the idea that CHOP treatment may indeed stimulate the development of effective anti-tumor immunity [30].

Increasing evidence indicates that the tumor microenvironment has critical roles in all aspects of cancer biology, including growth, angiogenesis, metastasis and progression. In this regard, it is recognized that chemokines and their receptors, originally identified as mediators of inflammatory diseases, serve as critical communication bridges between tumor cells and stromal cells to create a permissive microenvironment for tumor growth and metastasis [31–34]. In melanoma, it has been demonstrated that up regulation of expression of several chemokine genes such as *Ccl2*, *Ccl3*, *Ccl4*, *Ccl5*, *Cxcl9*, and *Cxcl10* in the tumor microenvironment correlates with the recruitment of activated effector T cells to the tumor increasing antitumor immunity [35]. Conversely, it has also been reported low amount of these chemokines in poorly infiltrated melanomas and colorectal carcinomas [35–37]. Our results showing a significant increase in *Ccl3*, *Ccl4*, *Ccl5* and *Cxcl9* genes expression in CHOPx2 group versus PBS group at day 45 p.t.i. are in accordance with those previously reported results, and confirm that in our model post-chemotherapy mice are fully immunocompetent. Furthermore, in CHOPx2 group we found a significant increase in *Cxcl12* expression but not in expression of its receptor *cxc4*. The CXCL12–CXCR4 biological axis has been associated

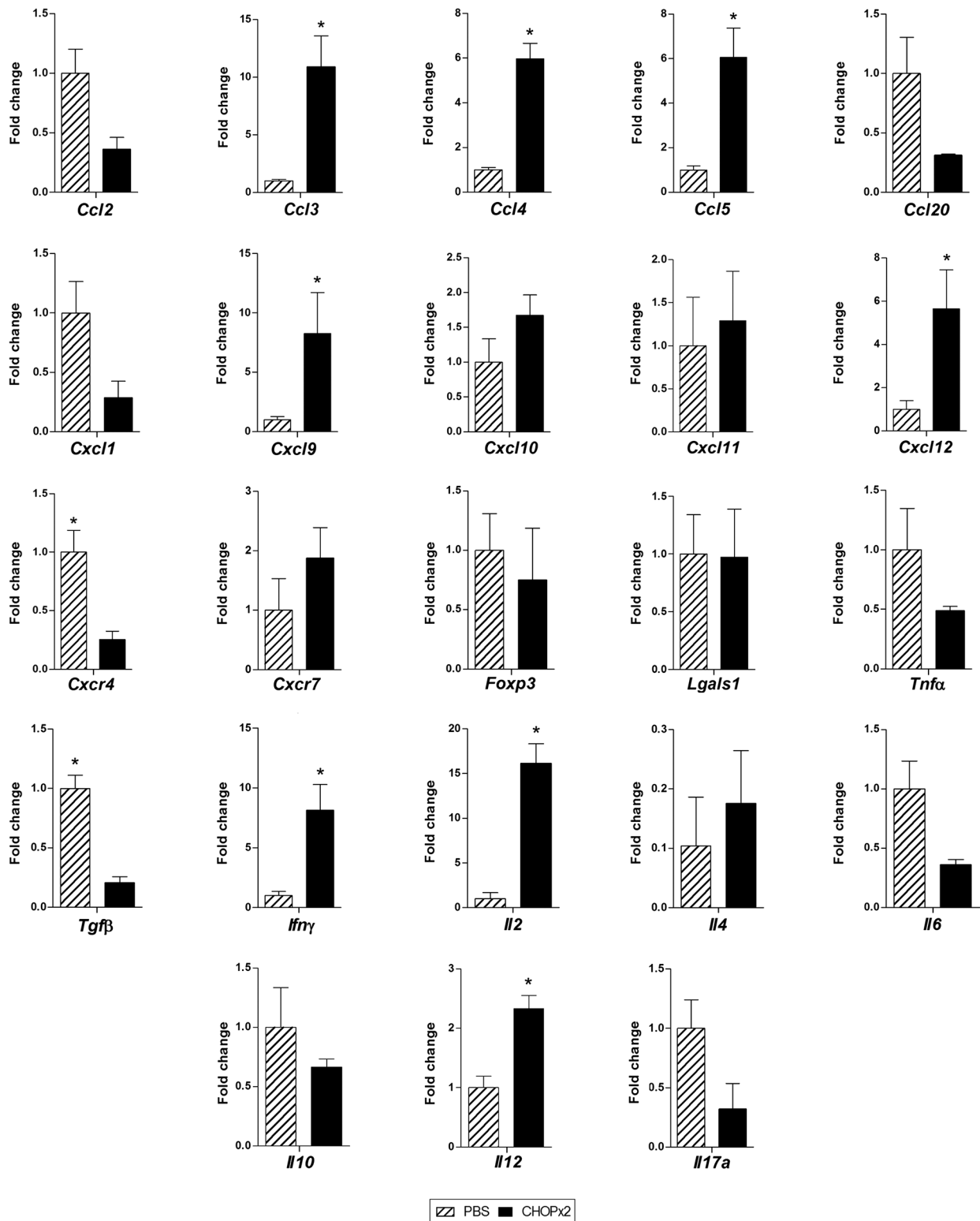


**Fig. 8** Cytokine/chemokine gene expression levels in the tumor microenvironment. Mice from PBS and CHOPx2 groups were sacrificed at day 45 p.t.i., and tumors were removed to assess the expression of cytokine and chemokines genes by quantitative RT-PCR on total tumor RNA. Gene mRNA values were normalized to that of *B2m* mRNA, and the results are expressed relative to mRNA levels in the PBS group. Results are shown as mean  $\pm$  standard deviation (n = 5). Significant differences were observed for *Ccl3*, *Ccl4*, *Ccl5*, *Cxcr4*, *Cxcl9*, *Cxcl12*, *Il2*, *Il12*, *Ifng* and *Tgfb* genes (p < 0.05)

with tumor invasion and metastases. In fact, CXCR4 is the most common chemokine receptor overexpressed in human cancer [32].

To confirm remission and monitored the disease an *in vivo* imaging system (PET) was applied in our model. When tumor cannot be detected clinically the use of PET post-chemotherapy allows a diagnosis of complete remission. PET is a minimal invasive technology easy to perform on anaesthetized mice, offering serial dynamic observations of tumor development in the same animal. In recent years, the use of PET in the diagnosis and monitoring of NHL patients, as well as other types of cancer, has increased [30, 38]. The most frequent radiotracer used in oncology is the glucose analogue FDG labelled with the positron-emitting radionuclide  $^{18}\text{F}$ . Several studies have demonstrated  $^{18}\text{F}$ -FDG increased uptake in most lymphomas, with a good correlation between intensity uptake, malignancy and proliferation activity [39]. Chaise et al. demonstrated the feasibility of PET using  $^{18}\text{F}$ -FDG in high-tumor burden A20 murine model [40]. In this study we could evaluate the treatment response detecting intra-abdominal lymphoma and hepatic involvement. There was a good correlation between PET images and histology. To the best of our knowledge, our study is the first to assess the value of FDG-PET for *in vivo* evaluation of post-chemotherapy remission in a murine NHL model. In patients, it is accepted that post-chemotherapy inflammatory reactions increase the rate of false positives results obtained with PET. To minimized this in NHL patient the PET scan should be performed after at least 3 weeks post-chemotherapy [41]. A meta-analysis performed by Zijlstra et al. revealed a pooled sensitivity and specificity of 72% (95% CI 61–82%) and 100% (95% CI 97–100%), respectively [42]. In our PET studies we reached a good sensitivity (85.7%) whereas specificity was 75%. The lower specificity results compared with data reported in human could be explained by the remaining inflammation at the time of our analysis.

Overall, we describe a NHL-B MRD syngeneic murine model as a novel tool to evaluate immunotherapies effectiveness as well as to study tumor microenvironment in relapse lymphoma. This model is unique in many aspects, inasmuch: (a) it uses fully immunocompetent mice; (b) remission is obtained by CHOP chemotherapy using the same cytostatic drugs that are the first line standard treatment for NHL in humans; (c) lymphoma complete remission is reached and maintained for a reasonable therapeutic window (20 days) where immunotherapies can be tested; (d) animals remains immunocompetent despite chemotherapy; (e) it uses an *in vivo* imaging system to follow disease evolution that correlates well with histology as gold standard.

## Conclusions

We have developed a novel pre-clinical model for NHL lymphoma that resembles more closely the situation found in humans, providing a therapeutic window where immunotherapies can be tested in conditions closer to those found in patients. We feel that the availability of such a model provides an important tool for evaluating new immunotherapies and will help to bridge the gap between pre-clinical models and clinical trials.

## Abbreviations

ANOVA: analysis of variance; AUC: area under the curve; BWC: body weight change; CFSE: 5(6)-carboxyfluorescein diacetate *N*-succinimidyl ester; CHOP: cyclophosphamide, doxorubicin, vincristine, steroids; CHOP×1: one cycle of CHOP regimen; CHOP×2: two cycles of CHOP regimen; ConA: concanavalin A; CRT: calreticulin; CSR: cancer statistics review; DAMPs: danger-associated molecular patterns; DLBCL: diffuse large B cell lymphoma; 3D-MLEM: 3D maximum likelihood expectation maximization; DMSO: dimethyl sulfoxide;  $^{18}\text{F}$ -FDG:  $^{18}\text{F}$ -2-Fluor-2-desoxy-D-glucosa;  $\text{IC}_{50}$ : half maximal inhibitory concentration; i.p: intraperitoneal; IPI: international prognostic index; MRD: minimal residual disease; NHL: non-Hodgkin lymphoma; NT: non-target tissue; PBS: phosphate-buffered saline; PET/CT: positron emission tomography/computed tomography; PI: propidium iodide; p.t.i: post-tumor implantation; ROC: receiver operating characteristic; RT-PCR: real time-polymerase chain reaction; s.c: subcutaneously; SEER: surveillance, epidemiology, and end results program; T: target tissue; Tregs: regulatory T cells; VOIs: volumes of interest.

## Authors' contributions

SG and JAC conceived and supervised the project, designed the experiments and analyzed the data. TB designed and performed the experiments, and analyzed data. MM, AM and MGK helped with the *in vivo* experiments and analysis of the data. LR, AP, PO and HE designed PET experiments, performed and analyzed PET data. JPP helped in performing and analysis of histology experiments. TB, SG and JAC wrote the manuscript. All authors contributed with enriching discussions. All authors read and approved the final manuscript.

## Author details

<sup>1</sup> Departamento de Desarrollo Biotecnológico, Instituto de Higiene, Facultad de Medicina, UdelaR, Montevideo, Uruguay. <sup>2</sup> Cátedra de Hematología, Hospital de Clínicas, Facultad de Medicina, UdelaR, Montevideo, Uruguay. <sup>3</sup> Área de Investigación y Desarrollo, Departamento Biomédico, Centro Uruguayo de Imagenología Molecular (CUDIM), Montevideo, Uruguay. <sup>4</sup> Área de Patología Funcional y Morfológica, Departamento de Patología, Facultad de Veterinaria, UdelaR, Montevideo, Uruguay.

## Acknowledgements

The authors are indebted with B.N. Carlos Chavez and B.N. Nancy Seiler for chemotherapy reconstitution in the Chemotherapy Preparation Area available in the Hospital de Clínicas, Montevideo, Uruguay. We also thank B.Sc. Lucía Blixen for her valuable contribution in imaging edition and Guy Tejedor (Animal Facility, Instituto de Higiene) for excellent technical assistance.

## Competing interests

The authors declare that they have no competing interests.

## Availability of data and materials

All raw data supporting our findings is available on request.

## Ethics approval

All protocols for animal experimentation were carried out in accordance with procedures authorized by the Comisión Nacional de Experimentación Animal (CNEA), from Uruguay, to whom this work was previously submitted.

## Funding

This work was supported by a grant of the Agencia Nacional de Investigación e Innovación (ANII) (FMV\_1\_2011\_1\_7181), Uruguay. T.B. was supported by PEDECIBA and received a fellowship from ANII.

Received: 22 July 2016 Accepted: 4 November 2016

Published online: 22 November 2016

## References

- Zelenetz AD, Gordon LI, Wierda WG, Abramson JS, et al. Non-Hodgkin's lymphomas. Version 4.2014. In: NCCN Clinical Practice Guidelines in Oncology (NCCN Guidelines). National comprehensive cancer network; 2014. <https://www.nccn.org/about/nhl.pdf>. Accessed 20 Jun 2016.
- Howlander N, Noone AM, Krapcho M, Garshell J, Miller D, Altekruse SF, Kosary CL, Yu M, Ruhl J, Tatalovich Z, Mariosio A, Lewis DR, Chen HS, Feuer EJ CK, editors. SEER cancer statistics review, 1975–2012, National Cancer Institute. [http://seer.cancer.gov/csr/1975\\_2012/](http://seer.cancer.gov/csr/1975_2012/).
- Zappasodi R, de Braud F, Di Nicola M, Koeck S, Zwierzina M, Huber JM, et al. Lymphoma immunotherapy: current status. *Front Immunol*. 2015;6:448.
- Farkona S, Diamandis EP, Blasutig IM. Cancer immunotherapy: the beginning of the end of cancer? *BMC Med*. 2016;14:73.
- Baio FE, Kwak LW, Weng J. Towards an off-the-shelf vaccine therapy targeting shared B-cell tumor idiotypes. *Am J Blood Res*. 2014;4:46–52.
- Ledford H. Translational research: 4 ways to fix the clinical trial. *Nature*. 2011;477:526–8.
- Bocchia M, Bronte V, Colombo MP, De Vincentiis A, Di Nicola M, Forni G, et al. Antitumor vaccination: where we stand. *Haematologica*. 2000;11:1172–206.
- Mak IW, Evaniew N, Ghert M. Lost in translation: animal models and clinical trials in cancer treatment. *Am J Transl Res*. 2014;6:114–8.
- Donnou S, Galand C, Touitou V, Sautès-Fridman C, Fabry Z, Fisson S. Murine models of B-cell lymphomas: promising tools for designing cancer therapies. *Adv Hematol*. 2012;2012:1–13.
- Grille S, Brugnini A, Nese M, Corley E, Falkenberg FW, Lens D, et al. A B-cell lymphoma vaccine using a depot formulation of interleukin-2 induces potent antitumor immunity despite increased numbers of intratumoral regulatory T cells. *Cancer Immunol Immunother*. 2010;59:519–27.
- Grille S, Moreno M, Brugnini A, Lens D, Chabalgoity JA. A therapeutic vaccine using *Salmonella*-modified tumor cells combined with interleukin-2 induces enhanced antitumor immunity in B-cell lymphoma. *Leuk Res*. 2013;37:341–8.
- Grille S, Moreno M, Bascuas T, Marqués JM, Muñoz N, Lens D, et al. *Salmonella enterica* serovar *Typhimurium* immunotherapy for B-cell lymphoma induces broad antitumor immunity with therapeutic effect. *Immunology*. 2014;143:428–37.
- Agorio C, Schreiber F, Sheppard M, Fernandez M, Martinez MA, Chabalgoity JA. Live attenuated *Salmonella* as a vector for oral cytokine gene therapy in melanoma. *J Gene Med*. 2007;9:416–23.
- Gordon LI, Harrington D, Andersen J, Colgan J, Glick J, Neiman R, Mann R, Resnick GD, Barcos M, Gottlieb A, et al. Comparison of a second-generation combination chemotherapeutic regimen (m-BACOD) with a standard regimen (CHOP) for advanced diffuse non-Hodgkin's lymphoma. *N Engl J Med*. 1992;327:1342–9.
- Tsukihara H, Nakagawa F, Sakamoto K, Ishida K, Tanaka N, Okabe H, et al. Efficacy of combination chemotherapy using a novel oral chemotherapeutic agent, TAS-102, together with bevacizumab, cetuximab, or panitumumab on human colorectal cancer xenografts. *Oncol Rep*. 2015;33:2135–42.
- Hovhannisyan N, Guillouet S, Fillesoye F, Dhilly M, Patin D, Galateau F, et al. Evaluation of the specificity of [18F]fludarabine PET/CT in a xenograft model of follicular lymphoma: comparison with [18F]FDG and impact of Rituximab therapy. *EJNMMI Res*. 2015;5:23.
- Livak KJ, Schmittgen TD. Analysis of relative gene expression data using real-time quantitative PCR and the  $2^{-\Delta\Delta CT}$  method. *Methods*. 2001;25:402–8.
- Dijoseph JF, Dougher MM, Evans DY, Zhou BB, Damle NK. Preclinical anti-tumor activity of antibody-targeted chemotherapy with CMC-544 (inotuzumab ozogamicin), a CD22-specific immunoconjugate of calicheamicin, compared with non-targeted combination chemotherapy with CVP or CHOP. *Cancer Chemother Pharmacol*. 2011;67:741–9.
- Mohammad RM, Al-katib A, Aboukameel A, Sarkar F, Kucuk O. Genistein sensitizes diffuse large cell lymphoma to CHOP (cyclophosphamide, doxorubicin, vincristine, prednisone) chemotherapy. *Mol Cancer Ther*. 2004;2:1361–8.
- Ostrand-Rosenberg S. Animal models of tumor immunity, immunotherapy and cancer vaccines. *Curr Opin Immunol*. 2004;16:143–50.
- van Marion DMS, Domanska UM, Timmer-Bosscha H, Walenkamp AME. Studying cancer metastasis: existing models, challenges and future perspectives. *Crit Rev Oncol Hematol*. 2016;97:107–17.
- Emens LA, Middleton G. The interplay of immunotherapy and chemotherapy: harnessing potential synergies. *Cancer Immunol Res*. 2015;3:436–43.
- Sakamaki I, Qin H, Kwak LW. Translational development of vaccination strategies in follicular NHL. *Best Pract Res Clin Haematol*. 2011;24:295–304.
- Schuster SJ, Neelapu SS, Gause BL, Janik JE, Muggia FM, Gockerman JP, et al. Vaccination with patient-specific tumor-derived antigen in first remission improves disease-free survival in follicular lymphoma. *J Clin Oncol*. 2011;29:2787–94.
- Izutsu K. Treatment of follicular lymphoma. *J Clin Exp Hematol*. 2014;10:31–7.
- Coleman M, Lammers PE, Ciceri F, Jacobs IA. Role of Rituximab and Rituximab biosimilars in diffuse large B-cell lymphoma. *Clin Lymphoma Myeloma Leuk*. 2016;16:175–81.
- Nowak AK, Robinson BWS, Lake RA. Synergy between chemotherapy and immunotherapy in the treatment of established murine solid tumors. *Cancer Res*. 2003;63:4490–6.
- Chen G, Emens LA. Chemoimmunotherapy: reengineering tumor immunity. *Cancer Immunol Immunother*. 2013;62:203–16.
- McDonnell AM, Lesterhuis WJ, Khong A, Nowak AK, Lake RA, Currie AJ, et al. Tumor-infiltrating dendritic cells exhibit defective cross-presentation of tumor antigens, but is reversed by chemotherapy. *Eur J Immunol*. 2014;45:1–11.
- El-Galaly TC, Hutchings M. Imaging of non-Hodgkin lymphomas: diagnosis and response-adapted strategies. In: Evens AM, Blum KA, editors. *Cancer treatment research*. Springer: International Publishing; 2015. p. 125–46.
- Keeley C, Mehrad B, Strieter RM. CXCL chemokines in cancer angiogenesis and metastases. *Adv Cancer Res*. 2010;106:91–111.
- Guo F, Wang Y, Liu J, Mok SC, Xue F, Zhang W. CXCL12/CXCR4: a symbiotic bridge linking cancer cells and their stromal neighbors in oncogenic communication networks. *Oncogene*. 2016;35:816–26.
- Guan X. Cancer metastases: challenges and opportunities. *Acta Pharm Sin B*. 2015;5:402–18.
- Tang H, Qiao J, Fu YX. Immunotherapy and tumor microenvironment. *Cancer Lett*. 2016;370:85–90.
- Harlin H, Meng Y, Peterson AC, Zha Y, Tretiakova M, Slingluff C, et al. Chemokine expression in melanoma metastases associated with CD8+ T-Cell recruitment. *Cancer Res*. 2009;69:3077–85.
- Coppola D, Nebozhyn M, Khalil F, Dai H, Yeatman T, Loboda A, et al. Unique ectopic lymph node-like structures present in human primary colorectal carcinoma are identified by immune gene array profiling. *Am J Pathol*. 2011;179:37–45.
- Messina JL, Fenstermacher DA, Eschrich S, Qu X, Berglund AE, Lloyd MC, et al. 12-Chemokine gene signature identifies lymph node-like structures in melanoma: potential for patient selection for immunotherapy? *Sci Rep*. 2012;2:765.
- Kostakoglu L, Cheson BD. Current role of FDG PET/CT in lymphoma. *Eur J Nucl Med Mol Imaging*. 2014;41:1004–27.
- Novelli S, Briones J, Flotats A, Sierra J. PET/CT assessment of follicular lymphoma and high grade B Cell lymphoma—good correlation with clinical and histological features at diagnosis. *Adv Clin Exp Med*. 2015;24:325–30.
- Chaise C, Itti E, Petegnief Y, Wirquin E, Copie-Bergman C, Farcet JP, et al. [F-18]-fluoro-2-deoxy-D-glucose positron emission tomography as a tool for early detection of immunotherapy response in a murine B cell lymphoma model. *Cancer Immunol Immunother*. 2007;56:1163–71.
- Juweid ME, Stroobants S, Hoekstra OS, Mottaghy FM, Dietlein M, Guermazi A, et al. Use of positron emission tomography for response assessment of lymphoma: consensus of the imaging subcommittee of international harmonization project in lymphoma. *J Clin Oncol*. 2007;25:571–8.
- Zijlstra JM, Lindauer-van der Werf G, Hoekstra OS, Hooft L, Huijgens PC. 18F-fluoro-deoxyglucose positron emission tomography for post-treatment evaluation of malignant lymphoma: a systematic review. *Haematologica*. 2006;91:522–9.